ACS APPLIED MATERIALS & INTERFACES

Research Article

www.acsami.org

Indium Diffusion and Native Oxide Removal during the Atomic Layer Deposition (ALD) of TiO_2 Films on InAs(100) Surfaces

Liwang Ye and Theodosia Gougousi*

Department of Physics, University of Maryland−Baltimore County (UMBC), Baltimore, Maryland 21250, United States

ABSTRACT: A thermal atomic layer deposition (ALD) process with tetrakis-(dimethylamino) titanium and H_2O as reagents has been used to deposit TiO_2 films on native oxide and etched InAs(100) surfaces at 200 °C. TiO_2 was deposited on etched InAs(100) surface without the formation of undesirable interfacial layers. X-ray photoelectron spectroscopy (XPS) data on a series of films of increasing thickness deposited on surfaces covered with native oxide has shown that the surface arsenic oxides are removed within the first 2−3 nm of film deposition. The indium oxides, however, after an initial reduction seem to persist and increase in intensity with film thickness. For a 6.4-nm-thick TiO_2 film, XPS depth profile data demonstrate an accumulation of indium oxides at the TiO_2 film surface. When the topmost layer of the indium/TiO_2 film is removed, then a sharp interface between the TiO_2 film and the InAs substrate is detected. This observation demonstrates that the surface oxides diffuse through fairly thick TiO_2 films and may subsequently be removed by reaction with the precursor and amine byproducts of the ALD reaction. These findings underscore the importance of diffusion in understanding the so-called "interface clean-up" reaction and its potential impact on the fabrication of high-quality InAs and other Group III−V-based MOS devices.

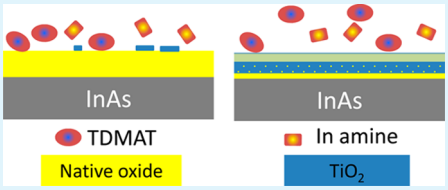

KEYWORDS: *indium arsenide, interface "clean-up", diffusion, atomic layer deposition, indium oxides*

INTRODUCTION

Atomic layer deposition (ALD) has gained widespread interest in the past decade as a thin-film deposition technique that enables deposition of high-quality thin films with precise thickness control.[1] Current understanding of the atomic level reaction mechanisms relies on a simplified picture based on surface functionalization and a ligand exchange mechanism. Recent experimental results and computational approaches have shown that this simplified picture is not always valid, and, in most cases, even for Si surfaces, there are several competing reactions that must be considered.[2−8]

Although Group III−V semiconductors such as GaAs and InAs have superior electrical properties to Si, the absence of a high-quality native oxide has prevented their widespread use in modern electronic devices. Control of the interface oxidation and passivation is a prerequisite for the fabrication of high-quality devices. The advent of ALD has provided a well-established approach for the deposition of a high-quality oxide on a variety of surfaces. Coupled with the development of stable surface passivation approaches, interest in fabrication of devices on Group III−V semiconductors has increased.[9−12] ALD of metal oxides on native oxide Group III−V surfaces have been shown to result, in addition to the deposition of a film, in the removal of a substantial amount of the surface native oxides as well, in stark contrast to depositions on Si where, invariably, the deposition of the film is accompanied by the formation of 1−2 nm of interfacial SiO_2. Most of the precursors associated with this "clean-up" effect are amines with the metal atoms being hafnium, titanium, or tantalum.[13−17] Deposition of Al_2O_3 from TMA and H_2O has been shown to result also in native oxide removal; however, based on recent computational and experimental results, it is believed that that the atomic-level mechanism is different than in the case of the alkylamides.[2,4,18,19] ALD reactions on Group III−V semiconductors are especially hard to model, because the surface chemistry is very complex; each of the constituent oxides has multiple oxidation states, and reactions between the surface oxides and the substrate are possible. Consequently, experimental results are needed to guide the theory by elucidating the relative importance of the various processes including diffusion and mixing of the surface native oxide through the deposited film.

In this work, we study the deposition and interface structure of TiO_2 films on native oxide and etched InAs(100) surfaces. We demonstrate that the surface indium oxides diffuse through ∼7 nm of TiO_2 film to accumulate near the surface of the film leaving behind a practically sharp interface. This observation provides insight into the "clean-up" mechanism showing the gradual and continuous removal of the surface oxides that is predominant for ALD processes utilizing amine precursors.[16,20]

EXPERIMENTAL METHODS

The samples were prepared using a home-built ALD reactor described elsewhere.[21] The films were deposited from the reaction of tetrakis(dimethylamino) titanium [$Ti(N(CH_3)_2)_4$] (TDMAT) with H_2O at 200 °C. The flow tube pressure was ∼220 mTorr during the deposition, and the typical pulse pressure heights for the TDMAT and H_2O were ∼5−10 mTorr and 20 mTorr, respectively, as measured by a capacitance manometer. These conditions represent the optimal

Received: June 4, 2013
Accepted: July 29, 2013
Published: July 29, 2013

   dx.doi.org/10.1021/am402161f | ACS Appl. Mater. Interfaces 2013, 5, 8081−8087

deposition temperature for the specific reagents in our reactor geometry, and the growth rate under these conditions was 0.42 Å/cy. Native oxide InAs(100) were the main surfaces studied and were used after successive rinses in acetone, methanol, and a final deionized (DI) water rinse and N_2 blow dry. Etched InAs surfaces were prepared via two different approaches. For both of them, the substrates were initially immersed in J.T. Baker 100 solutions[22] for 5 min, followed by a 5-min DI water rinse and N_2 blow dry. Surfaces marked "HF etched" were then etched in buffered oxide etch solutions for 20 s, followed by a quick DI water rinse, and N_2 blow dry. Surfaces marked "NH_4OH etched" were etched in ammonium hydroxide (28%−30%) solutions for 3 min, followed by a quick DI water rinse and N_2 blow dry. Etched samples were loaded into the deposition furnace quickly to minimize exposure to the ambient and possible surface reoxidation. During every deposition, a companion native oxide Si(100) sample was placed in the reactor to facilitate TiO_2 film thickness measurement via spectroscopic ellipsometry (J.A. Woollam alpha-SE) and to ensure process reproducibility.

Most of the samples were grown thin enough that the interface could be characterized using ex situ X-ray photoelectron spectroscopy (XPS), using a Kratos AXIS 165 spectrometer with an Al X-ray source (1486.7 eV) that was equipped with a 165-mm radius hemispherical analyzer and an 8-channeltron detection system. The samples were kept in a well-sealed desiccator to minimize the effect of air exposure prior to analysis. Argon-ion sputtering was used for depth profiling. During sputtering, the chamber pressure was ~5×10^{-7} Torr and the ion gun was operated at 4 kV and 1 mA. The ion beam was rastered across the sample at an angle of incidence of 54°. Unless specifically stated, the samples did not undergo any sputter cleaning prior to analysis. Data were collected for the core electrons from two regions for As (As 3d and As 3p) and In (In $3d_{5/2}$ and In 4d) at a step size of 0.1 eV, pass energy of 20 eV, and with photoelectron emission normal to the sample surface. A combination of Shirley and linear background was used for baseline correction. Each spectral region was analyzed using Gaussian−Lorentzian line mixtures; the Lorentzian peak full width at half-maximum (fwhm) was set at 40% of the Gaussian fwhm for all peaks. Spin orbits splitting and binding energies were taken from refs 17 and 23−25. To make the analysis consistent, all the samples for the same regions were fitted with the same binding energy and fwhm, except for the sputtered samples; these lines were significantly broadened.

Transmission electron imaging of the samples both in the bright field (Philips EM420), and high-resolution modes (FEI Tecnai) were provided by TEM Analysis Services Lab. The electron energy for the HRTEM and bright-field modes were 200 keV and 120 keV, respectively. Conventional TEM sample preparation methods including Ar-ion beam milling were used for sample preparation.

RESULTS

As-received InAs(100) wafers are covered with a thin layer of native oxide. HRTEM data presented in Figure 1 show that there is little variation of the oxide thickness locally, and the average measured thickness is 1.6 ± 0.1 nm. XPS analysis of such surfaces (Figure 2) has shown them to be indium-rich,

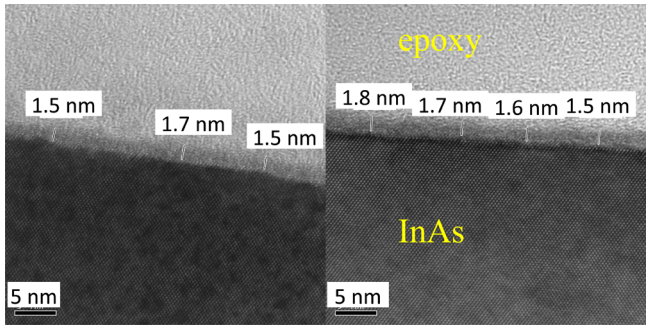

Figure 1. HRTEM images of an as received InAs(100) surface covered with native oxide. The mean value of the oxide thickness was measured at 1.6 ± 0.1 nm.

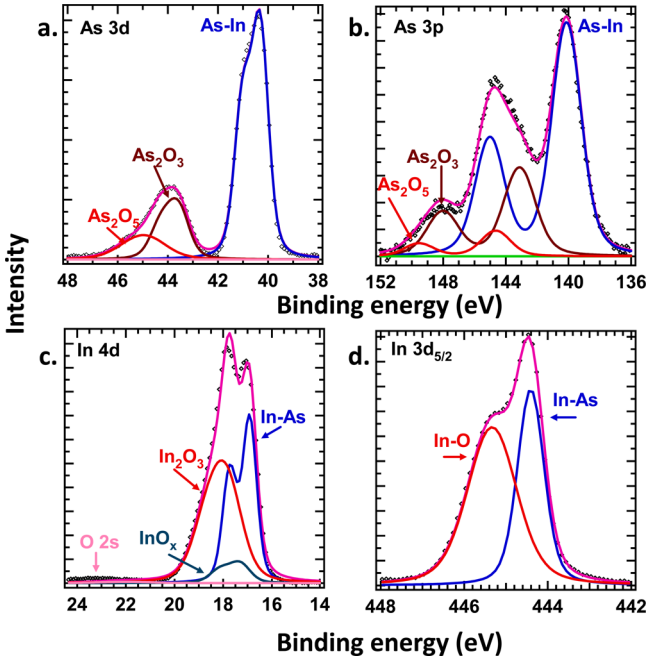

Figure 2. (a) As 3d, (b) As 3p, (c) In 4d, and (d) In $3d_{5/2}$ XPS spectra for the InAs(100) surface native oxide. The native oxides consist of a mixture of arsenic oxides (As_2O_3 and As_2O_5) and indium oxides (In_2O_3 and InO_x).

with a mixture of arsenic (As_2O_3 and As_2O_5) and indium (In_2O_3 and InO_x) oxidation states present. All indium and arsenic oxides peaks were separated in their components, except for the In $3d_{5/2}$ region, which was treated as one peak, since an insufficient amount of information exists in the literature for the exact binding energies of the various components.

A first set of depositions was performed on etched InAs surfaces, and, in Figure 3, we present the high-resolution XPS spectra for the As and In regions for a 2.2-nm-thick TiO_2 film. The two films were deposited side by side to facilitate comparison and minimize the effects of process variations. In both cases, a practically sharp interface is observed, no arsenic oxide and only traces of indium oxides are detected, in agreement with other ALD depositions on Group III−V surfaces.[16,26] Assuming that the indium oxide is located at the interface, and combining the ratio of oxide to the substrate area for both the In 4d and In $3d_{5/2}$ regions, an inelastic-mean-free path[27] of 3.4 nm for the In 4d and 2.6 nm for the In $3d_{5/2}$ and the TEM-based measurement of the native oxide layer thickness, then the thicknesses of the indium oxide can be estimated at ~0.2−0.3 nm, or about a monolayer. In addition to demonstrating that TiO_2 depositions on etched InAs surfaces can result in an abrupt interface, this set of data proves that, at ~2 nm, the TiO_2 film is sufficiently thick to protect the integrity of the interface from post-deposition oxidation. The traces of indium oxide observed are more likely due to incomplete removal of the native oxide, rather than post-deposition oxidation; such an occurrence would have resulted in a mixture of both arsenic and indium oxides, which is contrary to our observations. Based on this observation, the

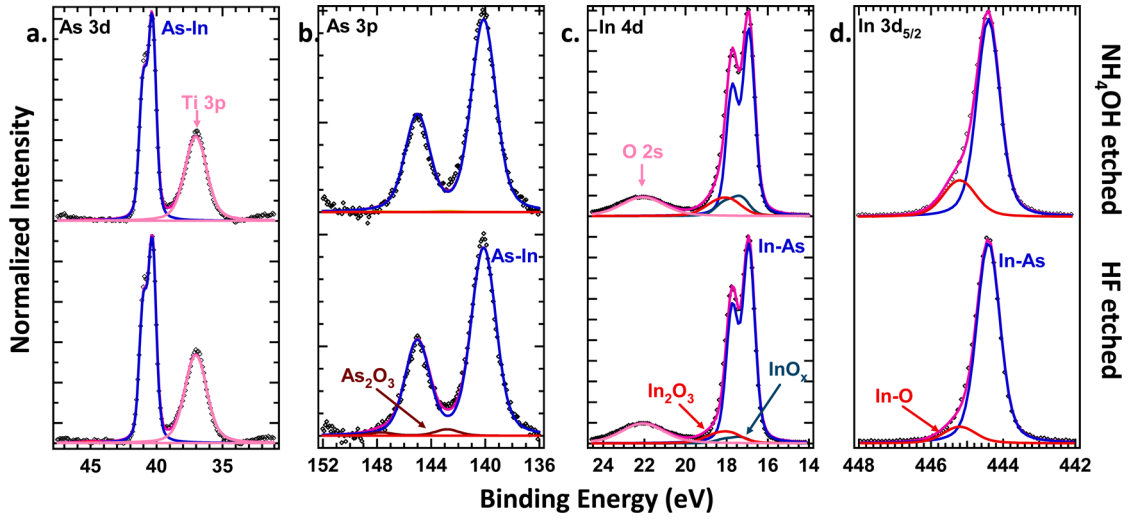

Figure 3. (a) As 3d, (b) As 3p, (c) In 4d, and (d) In $3d_{5/2}$ high-resolution XPS spectra for 2.2 nm of TiO_2 deposited on InAs surfaces that have been etched in either NH_4OH(top) or HF (bottom). A practically sharp interface is obtained in both instances with only traces of In and As oxides detected.

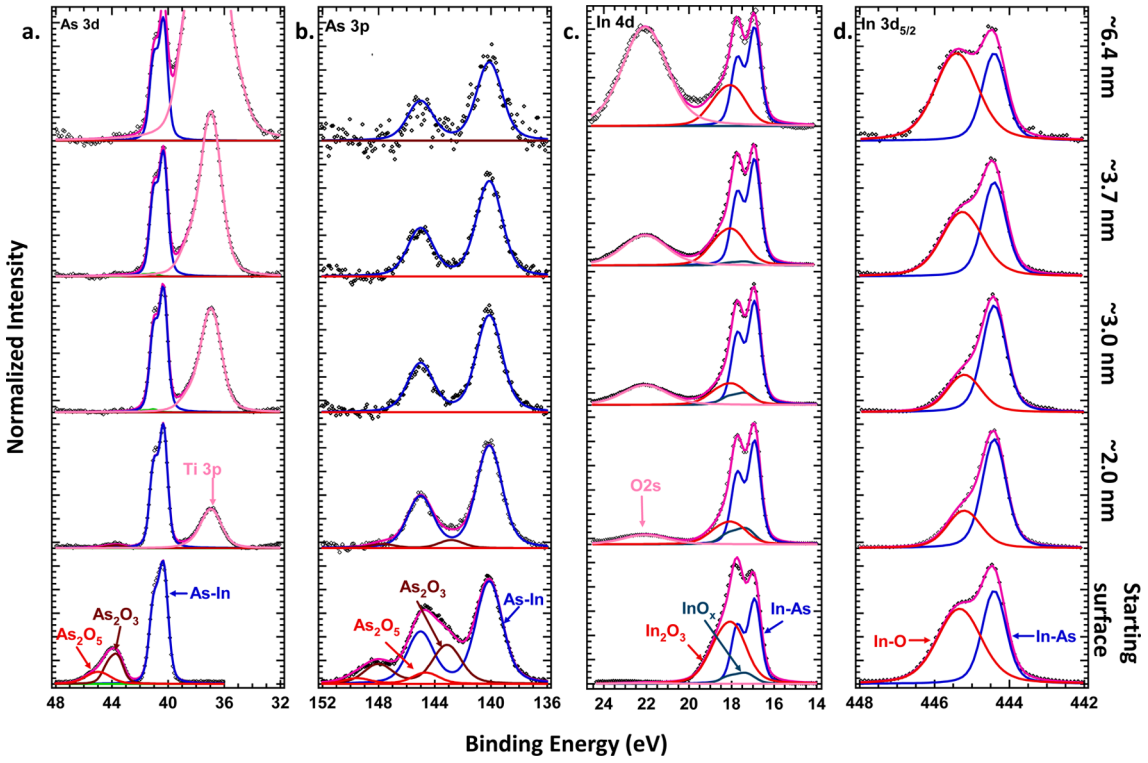

Figure 4. (a) As 3d, (b) As 3p, (c) In 4d, and (d) In $3d_{5/2}$ high-resolution XPS spectra for a series of TiO_2 films deposited on native oxide InAs surfaces. The spectra for the starting surface are also included to provide easy comparison. The arsenic oxides are barely detectable after the deposition of 2 nm of TiO_2. For the indium oxides, a reduction in their relative intensity is detected after the deposition of 2-nm and 3-nm films. However, for thicker films (3.7 and 6.4 nm), the intensity of the indium oxide peaks seems to increase.

remaining data presented in this manuscript will involve films thicker than 2 nm.

A series of TiO_2 films with thicknesses of 2−6.4 nm were deposited on native oxide InAs(100) surfaces and were analyzed using XPS. The spectra for several regions (As 3p, As 3d, In 4d, and In $3d_{5/2}$) are presented in Figure 4. In the same figure, we include the spectra taken for the starting surface, to facilitate comparison. Traces of arsenic oxides are detected for the 2-nm film while for the thicker films no arsenic oxides are present. For the indium oxides, a substantial reduction in their intensity is observed for the 2-nm films and the concentration of the oxides seems to remain unchanged for the 3-nm film. As the film thickness increases, the peaks associated with the indium oxides seem to increase in intensity. Since the signal intensity in XPS depends on the depth from which the photoelectrons originate, this observation can have two explanations:

(i) The thickness of the oxide layer increases with the increased deposition time as a result of interface

dx.doi.org/10.1021/am402161f | ACS Appl. Mater. Interfaces 2013, 5, 8081−8087

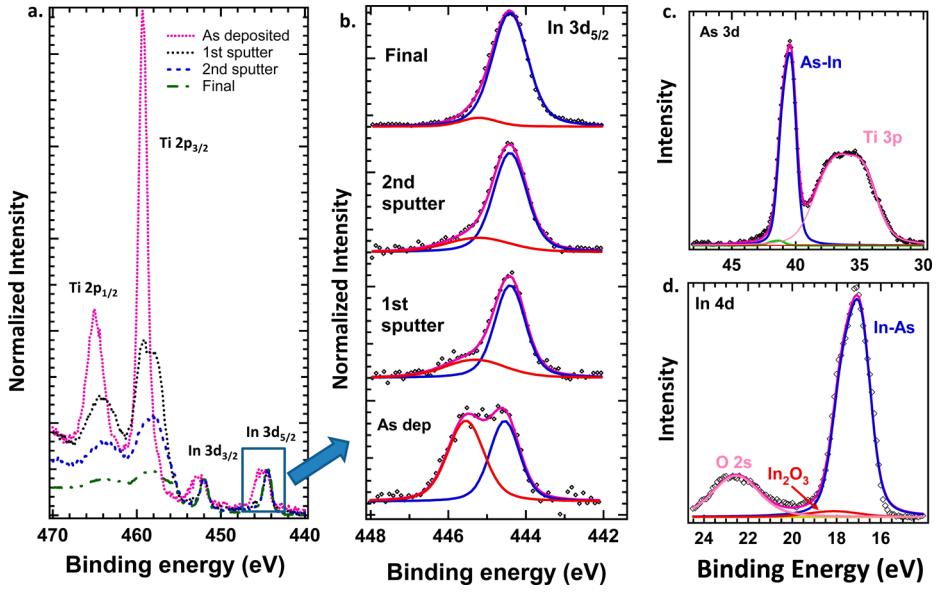

Figure 5. (a) In 3d and Ti 2p region spectra during depth profiling of a 6.4-nm-thick TiO_2 film deposited on native oxide InAs(100) surface. (b) Magnification of the In $3d_{5/2}$ region. Indium oxide seems to accumulate at the TiO_2 film surface. The As 3d spectra (panel (c)) and In 4d spectra (panel (d)) were acquired after the final sputter step and show that the interface is clean of arsenic oxides, with a very small amount of indium oxide still remaining. The As 3d region also includes signal from the Ti 3p electrons and shows that the TiO_2 has not been completely removed.

oxidation. Since this increase in the indium oxide peak intensity is not accompanied by a similar increase in the arsenic oxide peak intensity, this explanation is highly unlikely.

(ii) The indium oxides are mobile, diffuse through the TiO_2 film, and relocate close to the film surface. As signal attenuation in XPS is an exponential function of the depth, a small variation in the species location below the surface can affect the peak intensity substantially.

To test the second hypothesis, we used the Ar-ion beam in the XPS chamber to remove part of the TiO_2 film gradually and scanned the extended Ti 2p and In 3d region, as well as the In $3d_{5/2}$ region in high resolution. The depth profile was obtained at a later day from another piece of the same 6.4-nm-thick TiO_2 film used for Figure 4. Three depth profiles, in addition to the starting surface, were recorded and are presented in Figure 5. Figure 5a presents the extended spectral region that includes both Ti 2p and In 3d lines. The Ti 2p peaks allow for a visual inspection of the gradual TiO_2 removal. High-resolution scans of the In $3d_{5/2}$ regions for each depth is presented in Figure 5b. Combining the observations from both of these plots, one can see that the removal of the topmost layer of material (first sputter) results in reduction of the Ti 2p signal and significant decrease in the InO peak intensity, relative to the substrate peak. The next step (second sputter) removes more TiO_2 thickness and the relative intensity of the InO peak is further reduced. During those scans, a significant line broadening, characteristic of sputtered samples, is observed.[28,29] However, this broadening does not interfere with our observations. The final sputter step still leaves enough of the TiO_2 film in place to protect the buried interface, as evidenced by the Ti 3p peaks displayed in Figure 5c. The spectra from this ending scan show that the deposition of the 6.4 nm of TiO_2 on 1.6 nm of InAs native oxide results in a practically sharp interface that contains only traces on InO_x. All of the arsenic oxides have been removed during the deposition process, as evidenced both by the thickness series presented in Figure 4 and the final scan of the depth profile.

A sample of intermediate thickness of 4.3 nm of TiO_2 deposited on native oxide InAs was used to obtain cross-sectional bright-field and high-resolution transmission electron microscopy (HRTEM) data. Samples of the images for different magnifications are displayed in Figure 6. The bright-field images in Figures 6a and 6b shows a uniform film with no discernible contrast variation. The HRTEM images in Figures

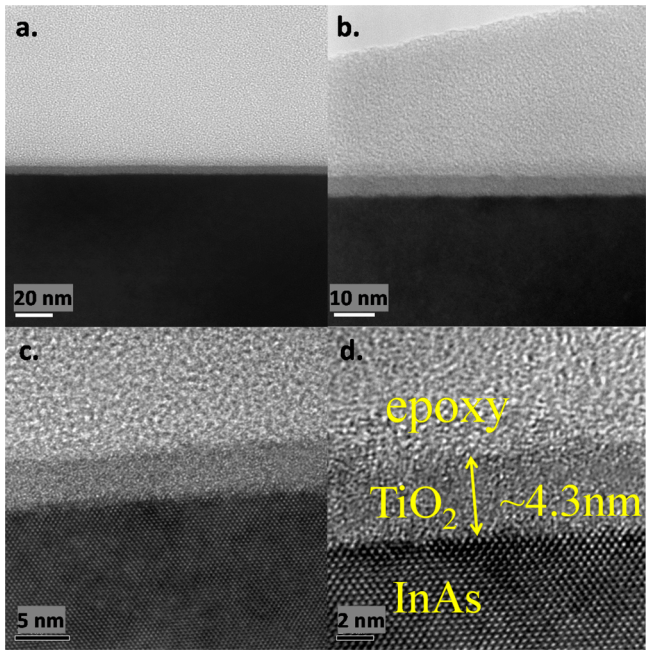

Figure 6. (a, b) Bright-field and (c, d) high-resolution transmission electron microscopy (HRTEM) data for a 4.3-nm TiO_2 film deposited on 1.6 nm of native oxide InAs(100) surface. The film is amorphous and free of pinholes.

6c and 6d verify this observation and additionally show the existence of a practically sharp interface, indicating the complete removal of the 1.6 nm of native oxide during the deposition process.

DISCUSSION

The ALD of TiO_2 on a 1.6-nm-thick layer of native oxide InAs(100) surfaces at 200 °C results in a practically sharp interface. Brennan and Hughes have shown that, for InGaAs surfaces, there is very little desorption of the indium oxides up to 400 °C, so we must attribute the observed removal of the surface indium oxides to the reactions occurring during the ALD process.[25] This observation mirrors many similar observations for the ALD of TiO_2 and other metal oxides on other Group III−V surfaces.[15−17,19,30] The common thread for most of these observations is the use of amine precursors, but a clear picture still has not emerged regarding the exact mechanism of the native oxide removal reaction. It is well-documented in the literature that the decomposition of species such as tris(dimethylamino) arsenic, trimethyl gallium, and tris(dimethylamino) antimony has been used for in situ removal of the surface native oxides from various Group III−V compound semiconductors, such as GaAs, InAs, and GaSb.[31−33] The high temperature (usually in excess of 450 °C) required for this process to be effective indicates that the fragmentation byproducts, which are mainly amines,[33] are responsible for the reaction. In ALD, extreme care is taken in preventing precursor fragmentation. As a result, for processes performed at the optimal ALD temperature, the only other active species besides the precursor can be the reaction byproducts. For the dimethyl amine precursors, these are usually amines, although other products also have been reported.

The fact that significant accumulation of InO_x is observed on the surface of a growing TiO_2 film and a sharp interface is buried underneath gives us significant insight on the indium oxide removal mechanism. Based on the data presented in Figures 4 and the depth profile of Figure 5, we can conclude that at least the removal of the indium oxides involves a multistep mechanism: when the surface oxides are accessible in the early cycles of the process, then there is direct reaction with the amine precursor and the amine reaction byproducts that result in the production of volatile species and as a result in the gradual removal of the indium oxides. However, clearly this does not remove all the surface oxides. Since the TiO_2 film grows in thickness and coalesces, this direct interaction is hindered. However, we have provided evidence that the indium oxides diffuse through the TiO_2 film. When they reach the top of the film, then they react with the amine precursor and the amine reaction byproducts to produce volatile species. A schematic for this mechanism is depicted in Figure 7. Diffusion and mixing of In^{3+} ions in films and TiO_2 more specifically is well-documented in the literature. Atanacio et al. have recently shown intermixing and significant diffusive transport of In_2O_3 in single-crystal rutile TiO_2 films.[34] In and Ga diffusion in InGaAs/InAlAs interfaces,[35] as well as diffusion of Ga atoms through HfO_2, has also been documented.[36] For interfaces and alloys containing In and Ti species, it has been shown that Ti has a high propensity to oxidize and In has a high propensity to reduce.[37,38] ALD reactions usually result in the formation of an almost-stoichiometric film, so this channel is only expected to be significant if titanium suboxides are produced.

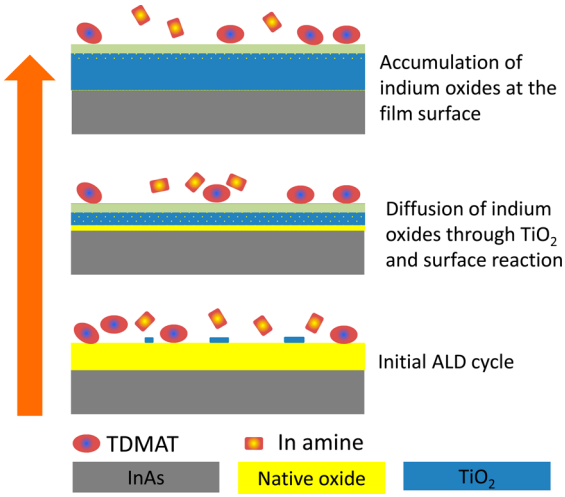

Figure 7. Schematic illustrating the proposed mechanism for the removal of the indium oxides during the ALD process: indium oxides diffuse through the TiO_2 films and react with the precursor and/or reaction byproducts to form volatile species.

The native oxides of the InAs(100) surface contain a combination of As_2O_3 and As_2O_5, as shown by the XPS analysis in Figure 2. Arsenic oxides are more volatile; however, generally, very little removal by desorption has been observed for vacuum anneals at 200 °C.[25,39] Deposition of ∼2 nm of TiO_2 results in the consumption of the majority of this native oxide, and for the 3.0-nm-thick film, no arsenic oxide is detected at the interface. There are several possible arsenic oxide consumption pathways, including a direct ligand substitution reaction with the precursor, reaction with the amine product of the ALD reaction, thermal desorption, and reaction with the substrate to produce more indium oxide (InO_x).[40]

$$As_2O_3 + 2InAs \rightarrow In_2O_3 + 4As$$

This surface reaction seems to be an important parameter in the arsenic oxide removal, because it is found to be more efficient for depositions under similar conditions on InAs(100) than GaAs(100). The detected accumulation of InO_x after the TiO_2 thickness reaches 3.0 nm also seems to agree with this.

There are several studies in the literature focusing on the interface "clean-up" during of ALD HfO_2 films on various InGaAs surfaces using amine precursors. Some of the authors show partial removal of the surface native oxide,[41−43] whereas, in other cases, a sharp interface is obtained.[44] Similarly, a gradual removal of the indium oxides has been shown by Dong et al. for deposition of HfO_2 on InP using a similar precursor.[18] C. H. Chang et al. have shown that, after deposition of a 7.4-nm-thick HfO_2 layer on 2.4 nm of native oxide $In_{0.15}Ga_{0.85}As$, using tetrakis(ethylmethylamino) hafnium at 200 °C, indium oxide was not detected on the surface of HfO_2 film, although traces of arsenic oxides were present.[44] Y. C. Chang et al. showed that, for a 7.8-nm-thick HfO_2 film deposited from the same precursor on 3.5−4 nm of native oxide $In_{0.53}Ga_{0.47}As$, native oxide was not detected on the film surface.[43] These observations may indicate that HfO_2 is more permeable to the indium oxides than TiO_2. For example, Kang et al. have recently demonstrated that gallium may diffuse very efficiently through ALD HfO_2 films, while Al_2O_3 seems to act as a diffusion barrier.[36] Further support to this explanation is provided by the demonstration that TiO_2 films act as effective

diffusion barriers in InGaAs/AlGaAs quantum well laser structures and suppress atom intermixing.[45]

Depositions of TiO_2 on etched surfaces show only traces of arsenic and indium oxides mirroring observations made on GaAs surfaces where the last monolayer of the gallium oxides seems to persist at the interface.[16,17] This observation is in sharp contrast with depositions of dielectrics on hydrogen terminated Si surfaces using similar ALD chemistries that results in the formation of 1−2 nm of interfacial SiO_2.[21] However, although devices can benefit from the existence of a sharp bottom interface, mixing of indium oxides in the dielectric may also result in lower effective dielectric constants and higher leakage currents.

CONCLUSIONS

Atomic layer deposition (ALD) of TiO_2 films from tetrakis-(dimethyl)amino titanium and H_2O at 200 °C on native oxide InAs(100) results in gradual consumption of the native surface and the formation of a sharp interface for sufficiently thick films. Arsenic oxides are consumed very quickly; ∼10% of the initial concentration remains after the deposition of 2 nm of film. Indium oxides seem to persist longer and are shown to diffuse through 5−7 nm of TiO_2 and accumulate at the film surface. The interface "clean-up" reaction observed is based on diffusion of the indium oxides to the film surface and subsequent removal through reaction with the precursor and the ALD reaction byproducts to form volatile species. For sufficiently thick films, the ALD process removes all native oxide but a monolayer of indium oxide from the interface. Traces of indium oxide at the interface are detected, even for depositions on etched surfaces. The mixing of indium oxides in the dielectric may affect the electrical and insulating properties of the films.

AUTHOR INFORMATION

Corresponding Author

*E-mail: gougousi@umbc.edu.

Notes

The authors declare no competing financial interest.

ACKNOWLEDGMENTS

Support by the National Science Foundation (NSF) (No. DMR-0846445) and the Center on Materials and Devices for Information Technology Research (CMDITR) (No. DMR-0120967) is acknowledged. We are grateful to Dr. Karen G. Gaskell from the XPS facility of the University of Maryland for assistance with the data acquisition and many helpful discussions.

REFERENCES

(1) George, S. M. *Chem. Rev.* **2010**, *110*, 111−131.
(2) Lin, J.-M.; Teplyakov, A. V.; Rodrigues-Reyes, J. C. F. *J. Vac. Sci. Technol. A* **2013**, *31*, 021401/1−021401/17.
(3) Shirazi, M.; Elliott, S. D. *Chem. Mater.* **2013**, *25*, 878−889.
(4) Klejna, S.; Elliott, S. D. *J. Phys. Chem. C* **2012**, *116*, 643−654.
(5) Elliott, S. D. *Semicond. Sci. Technol.* **2012**, *27*, 074008/1−074008/10.
(6) Weinreich, W.; Tauchnitz, T.; Polakowski, P.; Drescher, M.; Riedel, S.; Sundqvist, J.; Seidel, K.; Shirazi, M.; Elliott, S. D.; Ohsiek, S.; Erben, E.; Trui, B. *J. Vac. Sci. Technol.* **2013**, *31*, 01A123/1−01A123/11.
(7) Zaera, F. *J. Phys. Chem. Lett.* **2012**, *3*, 1301−1309.
(8) Clemens, J. B.; Chagarov, E. A.; Holland, M.; Droopad, R.; Shen, J.; Kummel, A. C. *J. Phys. Chem.* **2010**, *133*, 154704/1−154704/6.
(9) Takei, K.; Kapadia, R.; Fang, H.; Plis, E.; Krishna, S.; Javey, A. *Appl. Phys. Lett.* **2013**, *102*, 153513/1−153513/4.
(10) Trinh, H. D.; Brammertz, G.; Chang, E. Y.; Kuo, C. I.; Lu, C. Y.; Lin, Y. C.; Nguyen, H. Q.; Wong, Y. Y.; Tran, B. T.; Kakushima, K.; Iwai, H. *IEEE Electron Device Lett.* **2011**, *32*, 752−754.
(11) Wang, C.; Xu, M.; Gu, J.; Zhang, D. W.; Ye, P. D. *Electrochem. Solid-State Lett.* **2012**, *15*, H51−H54.
(12) Wang, W.; Hwang, J. C. M.; Xuan, Y.; Ye, P. D. *IEEE Trans. Electron Devices* **2011**, *58*, 1972−1978.
(13) Ye, P. D.; Wilk, G. D.; Yang, B.; Kwo, J.; Chu, S. N. G.; Nakahara, S.; Gossmann, H.-J. L.; Mannaerts, J. P.; Hong, M.; Ng, K. K.; Bude, J. *Appl. Phys. Lett.* **2003**, *83*, 180−182.
(14) Frank, M. M.; Wilk, G. D.; Starodub, D.; Gustafsson, T.; Garfunkel, E.; Chabal, Y. J.; Grazul, J.; Muller, D. A. *Appl. Phys. Lett.* **2005**, *86*, 152904/1−152904/3.
(15) Huang, M. L.; Chang, Y. C.; Chang, C. H.; Lee, Y. J.; Chang, P.; Kwo, J.; Wu, T. B.; Hong, M. *Appl. Phys. Lett.* **2005**, *87*, 252104/1−252104/3.
(16) Gougousi, T.; Lacis, J. W. *Thin Solid Films* **2010**, *518*, 2006−2009.
(17) Gougousi, T.; Ye, L. *J. Phys. Chem. C* **2012**, *116*, 8924−8931.
(18) Dong, H.; Brennan, B.; Zhernokletov, D.; Kim, J.; Hinkle, C. L.; Wallace, R. M. *Appl. Phys. Lett.* **2013**, *102*, 171602/1−171602/4.
(19) Milojevic, M.; Hinkle, C. L.; Aguirre-Tostado, F. S.; Kim, H. C.; Vogel, E. M.; Kim, J.; Wallace, R. M. *Appl. Phys. Lett.* **2008**, *93*, 252905/1−252905/3.
(20) Gougousi, T.; Hackley, J. C.; Lacis, J. W.; Demaree, J. D. *J. Electrochem. Soc.* **2010**, *157*, H551−H556.
(21) Hackley, J. C.; Gougousi, T.; Demaree, J. D. *J. Appl. Phys.* **2007**, *102*, 034101/1−034101/7.
(22) Cady, W. A.; Varadarajan, M. *J. Electrochem. Soc.* **1996**, *143*, 2064−2067.
(23) Trinh, H.; Chang, E. Y.; Wong, Y.; Yu, C.; Chang, C.; Lin, Y.; Nguyen, H.; Tran, B. *Jpn. J. Appl. Phys.* **2010**, *49*, 111201/1−111201/7.
(24) Zborowski, J. T.; Vigliante, A.; Moss, S. C.; Golding, T. D. *J. Appl. Phys.* **1996**, *79*, 8379−8383.
(25) Brennan, B.; Hughes, G. *J. Appl. Phys.* **2010**, *108*, 053516/1−053516/8.
(26) Kirk, A. P.; Milojevic, M.; Kim, J.; Wallace, R. M. *Appl. Phys. Lett.* **2010**, *96*, 202905/1−202905/3.
(27) Powell, C. J.; Jablonski, A. In *NIST Electron Inelastic-Mean-Free-Path Database*, Version 1.2, SRD 71, National Institute of Standards and Technology, Gaithersburg, MD, 2010.
(28) Grunthaner, F. J.; Grunthaner, P. J.; Vasquez, R. P.; Lewis, B. F.; Maserjian, J.; Madhukar, A. *J. Vac. Sci. Technol.* **1979**, *16*, 1443−1453.
(29) Hofmann, S.; Thomas, J. H. *J. Vac. Sci. Technol. B* **1983**, *1*, 43−47.
(30) Hinkle, C. L.; Sonnet, A. M.; Vogel, E. M.; McDonnell, S.; Hughes, G. J.; Milojevic, M.; Lee, B.; Aguirre-Tostado, F. S.; Choi, K. J.; Kim, H. C.; et al. *Appl. Phys. Lett.* **2008**, *92*, 071901/1−071901/3.
(31) Marx, D.; Asahi, H.; Liu, X. F.; Higashiwaki, M.; Villaflor, A. B.; Miki, K.; Yamamoto, K.; Gonda, S.; Shimomura, S.; Hiyamizu, S. *J. Cryst. Growth* **1995**, *150*, 551−556.
(32) Gonda, S.; Asahi, H.; Yamamoto, K.; Hidaka, K.; Sato, J.; Tashima, T.; Asami, K. *Appl. Surf. Sci.* **1998**, *130−132*, 377−381.
(33) Whitaker, T. J.; Martin, T.; Johnson, A. D.; Pidduck, A. J.; Newey, J. P. *J. Cryst. Growth* **1996**, *164*, 125−131.
(34) Atanacio, A. J.; Nowotny, J.; Prince, K. E. *Sep. Purif. Technol.* **2012**, *91*, 96−102.
(35) Baird, R. J.; Potter, T. J.; Kothiyal, G. P.; Battacharya, P. K. *Appl. Phys. Lett.* **1988**, *52*, 2055−2057.
(36) Kang, Y.-S.; Kim, D.-K.; Jeong, K.-S.; Cho, M.-H.; Kim, C. Y.; Chung, K.-B.; Kim, H.; Kim, D.-C. *ACS Appl. Mater. Interfaces* **2013**, *5*, 1982−1989.
(37) Choi, S.-H.; Jung, W.-S.; Park, J.-H. *Appl. Phys. Lett.* **2012**, *101*, 212105/1−212105/3.

(38) Ivey, D. G.; Ingrey, S.; Noel, J.-P.; Lau, W. M. *Mater. Sci. Eng., B* **1997**, *B49*, 66−73.
(39) Ingrey, S.; Lau, W. M.; McIntyre, N. S. *J. Vac. Sci. Technol. A* **1986**, *4*, 984−988.
(40) Schwartz, G. P.; Griffiths, J. E.; Gualtieri, G. J. *Thin Solid Films* **1982**, *94*, 213−222.
(41) Timm, R.; Fian, A.; Hjort, M.; Thelander, C.; Lind, E.; Andersen, J. N.; Wernersson, L.-E.; Mikkelsen, A. *Appl. Phys. Lett.* **2010**, *97*, 132904/1−132904/3.
(42) Kobayashi, M.; Chen, P. T.; Sun, Y.; Goel, N.; Majhi, P.; Garner, M.; Tsai, W.; Pianetta, P.; Nishi, Y. *Appl. Phys. Lett.* **2008**, *93*, 182103/1−182103/3.
(43) Chang, Y. C.; Huang, M. L.; Lee, K.-Y.; Lee, Y. J.; Lin, T. D.; Hong, M.; Kwo, J.; Lay, T. S.; Liao, C. C.; Cheng, K. Y. *Appl. Phys. Lett.* **2008**, *92*, 072901/1−072901/3.
(44) Chang, C.-H.; Chiou, Y.-K.; Chang, Y.-C.; Lee, K.-Y.; Lin, T.-D.; Wu, T.-B.; Hong, M.; Kwo, J. *Appl. Phys. Lett.* **2006**, *89*, 242911/1−242911/3.
(45) Gareso, P. L.; Buda, M.; Fu, L.; Tan, H. H.; Jagadish, C. *Appl. Phys. Lett.* **2004**, *85*, 5583−5585.